DOI:10.22337/2587-9618-2019-15-3-14-39

КОНСТРУКЦИИ ВЫСОТНОГО ЗДАНИЯ «ЛАХТА ЦЕНТР» В САНКТ-ПЕТЕРБУРГЕ

Е.А. Илюхина [1], С.И. Лахман [2], А.Б. Миллер [3], В.И. Травуш [2, 4]
[1] АО «Многофункциональный комплекс Лахта Центр», г. Санкт-Петербург, РОССИЯ
[2] ЗАО «Городской проектный институт жилых и общественных зданий», г. Москва, РОССИЯ
[3] ПАО «Газпром», г. Москва, РОССИЯ
[4] Российская академия архитектуры и строительных наук, г. Москва, РОССИЯ

Аннотация: Построенный в конце 2018 года небоскреб «Лахта Центр» высотой 462 метра, расположенный в городе Санкт-Петербурге на берегу Балтийского моря, является самым высоким зданием в Европе. Башня имеет 87 надземных этажей и 2 подземных этажа. В настоящей статье рассматриваются конструкции этого высотного здания, в частности, приводится информация о свайном основании, конструкциях подземной части, конструкциях надземной части, конструкциях сталежелезобетонных колонн, конструкциях перекрытий, кратко описаны проведенные расчеты строительных конструкций и определение некоторых видов нагрузок, аэродинамические испытания, инженерно-геологические исследования, испытания сталежелезобетонных колонн, стеклянные стойки, реализованная система мониторинга объекта.

Ключевые слова: высотное здание «Лахта Центр», строительные конструкции, сталежелезобетонные колонны, нагрузки и воздействия, расчетное обоснование, мониторинг

STRUCTURES OF THE HIGH-RISE BUILDING “LAKHTA CENTER” IN SAINT-PETERSBURG

Elena A. Ilyukhina [1], Sergey I. Lakhman [2], Alexey B. Miller [3], Vladimir I. Travush [2, 4]
[1] Joint Stock Company “Multifunctional complex Lakhta Center”, Saint-Petersburg, RUSSIA
[2] Close Joint Stock Company “Planning Institute of Residential and Public Buildings”, Moscow, RUSSIA
[3] Public Joint Stock Company Gazprom, Saint-Petersburg, RUSSIA
[4] Russian Academy of Architecture and Construction Sciences, Moscow, RUSSIA

Abstract: The “Lakhta Center” skyscraper that built up in Saint-Petersburg on the coast of Baltic sea at the end of 2018 is the highest building of Europe. The tower has 87 floors above the ground and 2 underground floors. The distinctive paper is devoted to structures of this skyscraper. Particularly piled foundation, building structures of the underground part (substructure), building structures of the aboveground part (building superstructure), designs of steel-reinforced concrete columns, design of slabs, structural analysis, some loads and impacts, aerodynamic tests, engineering-geological research, testing of steel-reinforced concrete columns, glass racks and structural health monitoring are under consideration.

Keywords: high-rise building “Lakhta Center”, building structures, steel-reinforced concrete columns, loads and impacts, structural analysis, structural-health monitoring

1. GENERAL INFORMATION

The Lakhta Center skyscraper (tower) that built up in Saint-Petersburg on the coast of Baltic sea at the end of 2018 is the highest building of Europe. The tower has 87 floors above the ground and 2 underground floors.

In the plan, the tower is pentagonal star, the beams of which go apart from the central core, the building takes twisted conical form. Slabs of the overlap made of five square “petals” interconnected by the circle central core. Through the height of the building square “petals” rotate around their own axes counterclockwise for 0.82 degree at each floor (Figures 1, 2, 3, 4).

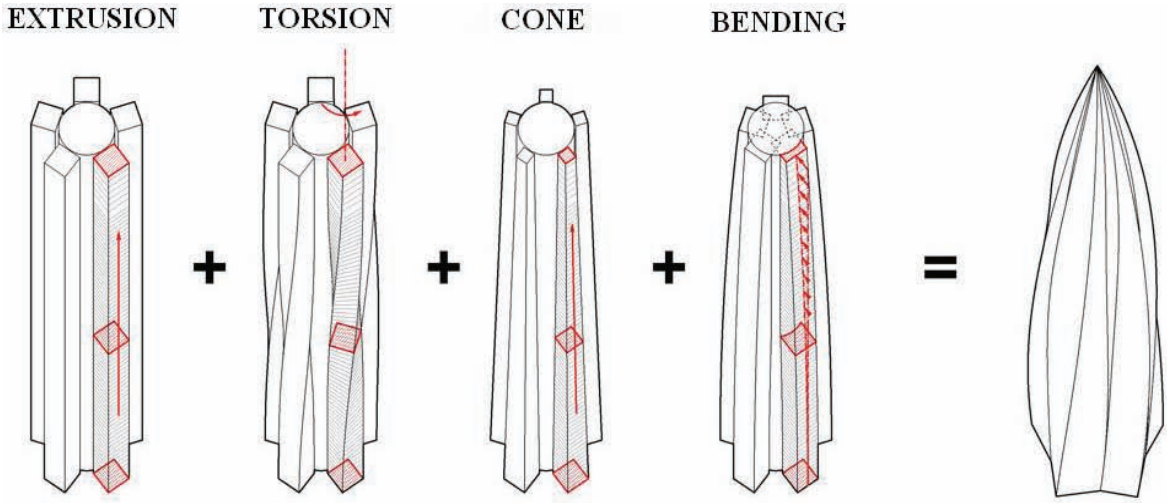

Figure 1. Scheme for obtaining of the tower geometry.

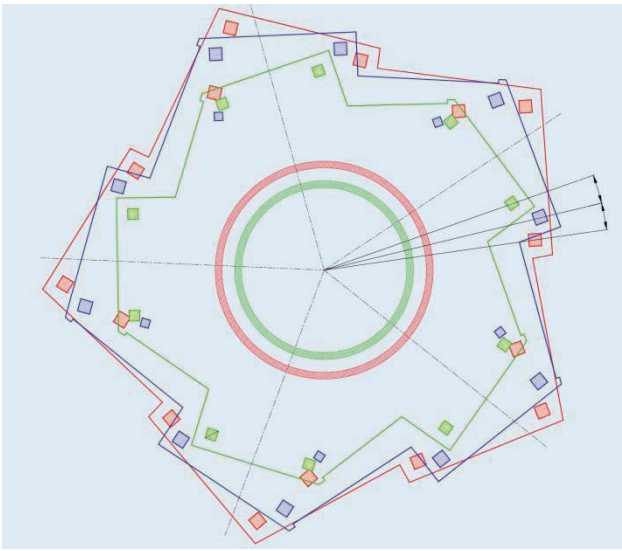

Figure 2. Combined plans of the 19, 39 and 59 floors.

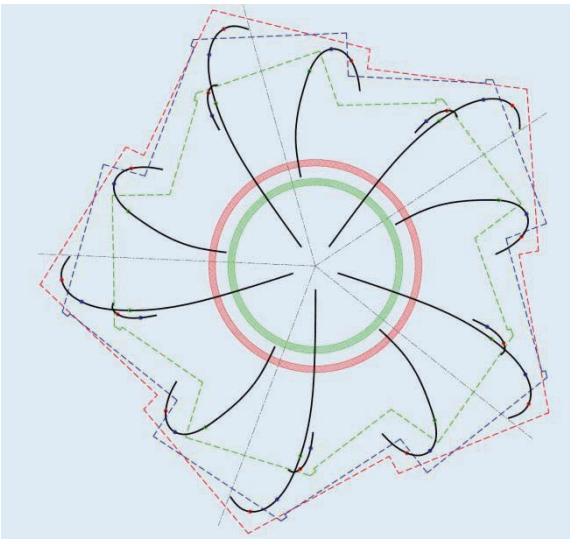

Figure 3. Combined plans of the 19, 39 and 59 floors.

Figure 4. General view.

2. PILED FOUNDATION

In accordance with results of geotechnical survey, the following layers are in the ground (from the top to the bottom, as it is shown in Figure 5):

- interlaminating weak layers of banded clays, sandy loam and sand (specimens 1-4);
- moraine (specimens 5,6);
- Vendian clay (specimens 7-9);
- Sandstone with layers of siltstone and mudstone (specimen 10).

Since the top layers of ground had low deformation modulus and strength, it was decided to use pile foundation supported on a Vendian clay. In order to decrease deflection of the foundation slab and efforts in the outer pile rows it were conducted calculations of pile field with different length of piles. As result, piled foundation of the tower consists of 264 bored piles of 2000 mm diameter and 55 or 65 m length, placed with step from 4 to 6 meters (Figure 6). Since piles were bored from ground surface, the fact depth of the piles were 72 and 82 m respectively (Figure 7).

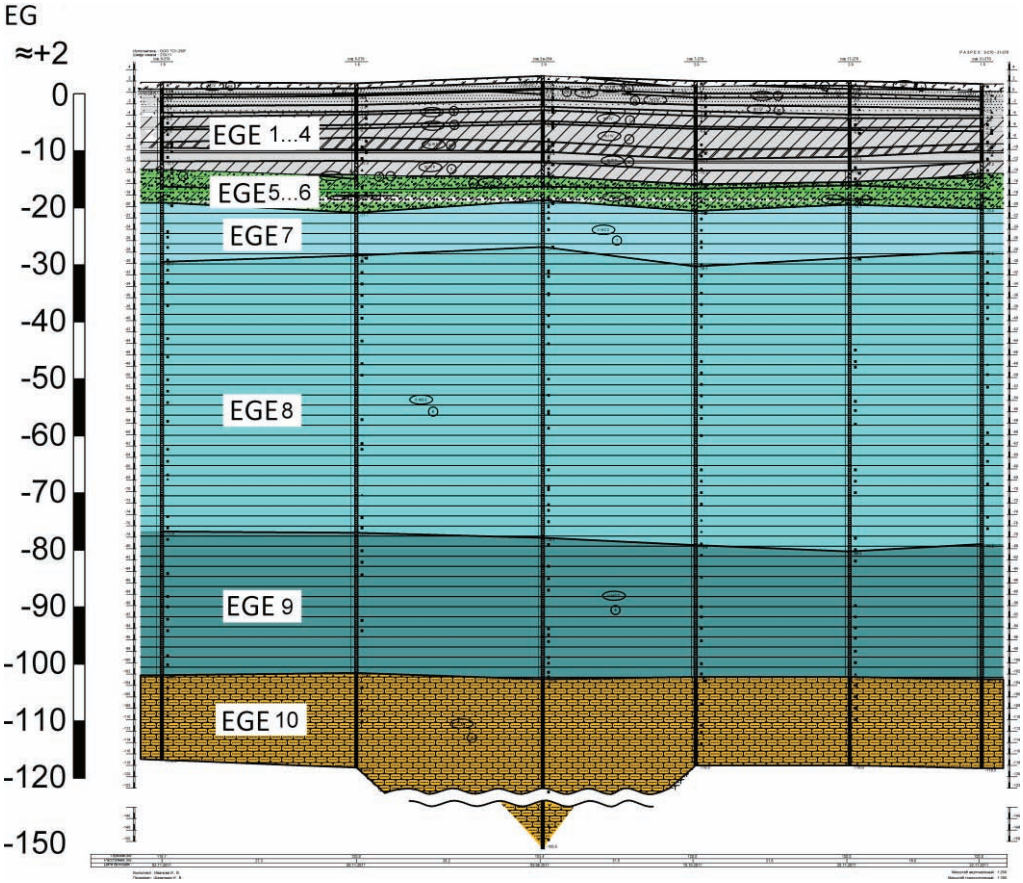

Figure 5. Layers of ground under the tower
(EGE – Engineering and geological element; EG – Existing grade).

Calculated loadbearing capacity of a pile of 55 m length was 36000 kN in accordance with regulatory documents and 64000 kN obtained by experiment. Calculated load bearing capacity of a pile of 65 m length was 43000 kN in accordance with regulatory documents and 77000 kN obtained by experiment. The average calculated loading on a pile was 25450 kN.

3. BUILDING STRUCTURES OF THE UNDERGROUND PART

The underground floors of the building in the plan have the shape of an equilateral pentagon with a length of each side 57.5 m. In the center of the building there is a central core with a down part diameter of 26.0 m.

The weight of the building from standard loads, including the weight of the box foundation, is 4,930,000 kN. Initial calculations to determine the required thickness of the foundation slab showed that, in order to obtain uniformity of sediments, a traditional foundation slab even 7-8 meters thick is not enough. The draft under the core was about 180 mm, while at the periphery the size of the draft was about 60 mm. Therefore, it was decided to create a box foundation that provided a more economical solution. The calculations showed that such a foundation has high rigidity (the difference in sediment between the core zone and the periphery does not exceed 25-30 mm), the average pressure under the base of the tower foundation from standard loads was 870 kPa.

The bottom plate, located at a relative mark of -17.650 m, has a thickness of 3600 mm, the top plate, located at a relative mark of -4.650 m, is made 2000 mm thick. The joint work of the lower and upper slabs of the box foundation is ensured by 10 stiffness diaphragms 2500 mm thick, diverging from the building core in the radial direction (Figures 7, 8).

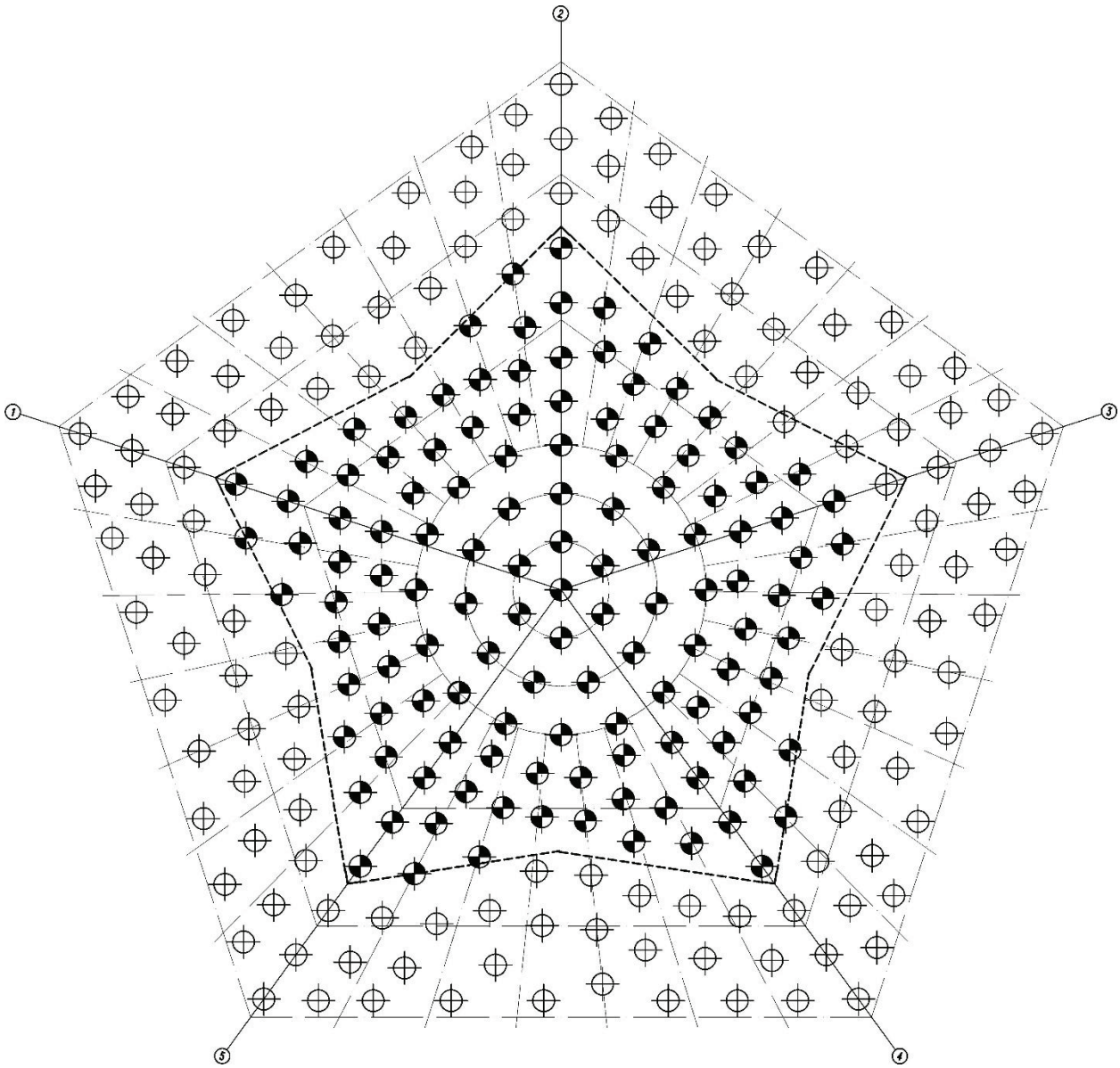

Figure 6. Piled foundation of the tower.

For the perception of large tensile forces, which amount to 23000 kN/m, the lower foundation plate is reinforced with 15 reinforcing meshes in height with rods with a diameter of 32 mm from A500C steel, spaced 150 mm apart. In the protective layers of the concrete slab at a distance of 25 mm from the upper and lower surfaces installed anti-shrink mesh with cells 100 x 100 mm. Between the upper and lower slabs of the box foundation there is a middle slab 0.4 m thick.

4. BUILDING STRUCTURES OF THE ABOVEGROUND PART

The underground part of the tower building is separated from the rest of the Lakhta Center complex by a sedimentary expansion joint. The aboveground part of the building at the 1st floor level is inscribed in a pentagon with a side length (between the axis of the columns) of 35.2 m (Figure 10). Up to the 16th floor, the dimensions of each subsequent floor of the aboveground part of the building increase.

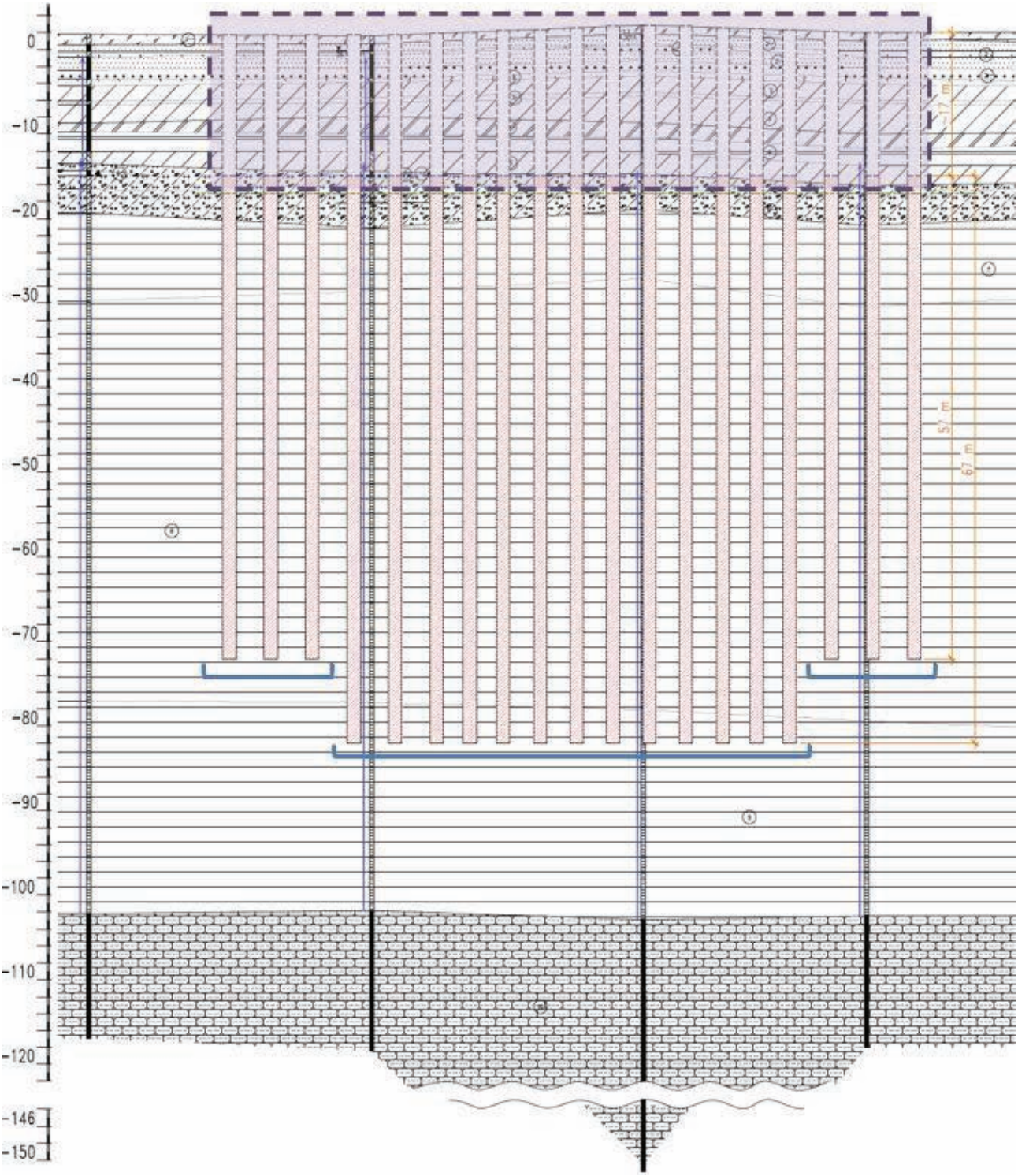

Figure 7. Piled foundation of the tower.

The maximum length of the side of the pentagon at the level of the 16th floor is 36.6 m. After the 16th floor, each subsequent floor of the aboveground part of the building is reduced in size. The length of the side of the pentagon at the level of the upper 86th floor is 19 m.

The structural scheme of the building is a core and frames.

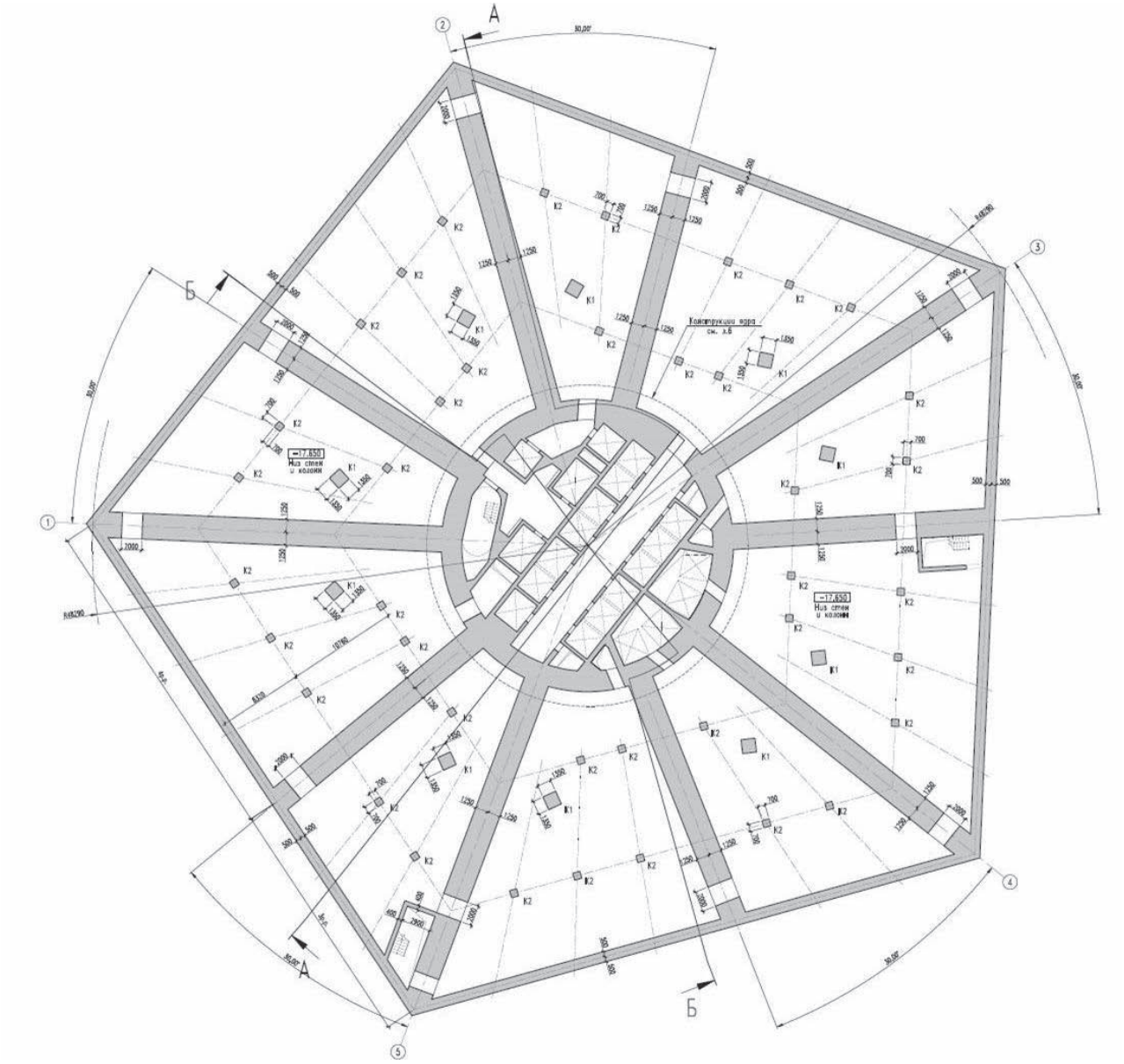

Figure 8. Walls and columns of the lower level of the box foundation of the tower.

The load bearing structures of the tower are the central reinforced concrete core and 10 steel-reinforced concrete columns around the perimeter. In order to reduce spans in the building, another 5 steel-reinforced concrete columns were introduced until the level of the 56th floor.

The central reinforced concrete core of a round shape is the main supporting structural element of the tower. The core perceives vertical and horizontal loads, including constant torsion caused by the shape of the building, and transfers them to the foundation.

The thickness of the outer walls of the core at -3 and -2 floors is 2500 mm, on the -1 and 1 floors it is 2000 mm, on the 2nd and 3rd floors it is 1700 mm, on the 4th and 5th floors it is 1400 mm, on the 6th and 7th floors it is 1100 mm, from 8 to 67 floors it is 800 mm, from 68 to 80 floors it is 600 mm, from 81 to 89 floors it is 400 mm. The thickness of the outer walls of the core is determined both by the calculation conditions for all types of impacts, and by the design requirements (the number and location of holes and openings, the multiplicity of the pitch of reinforcing meshes, etc.).

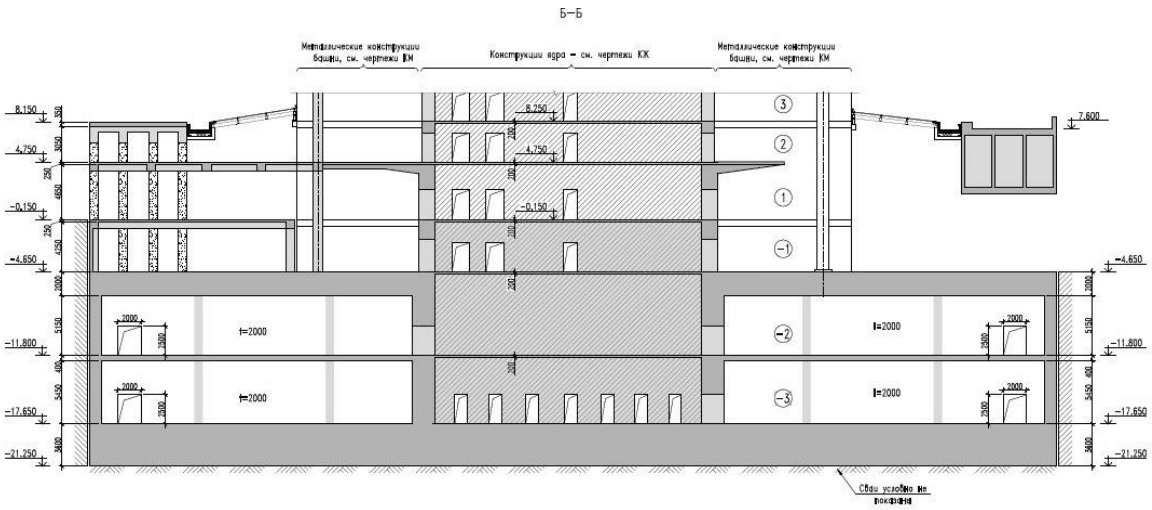

Figure 9. Structures of building core of the tower.

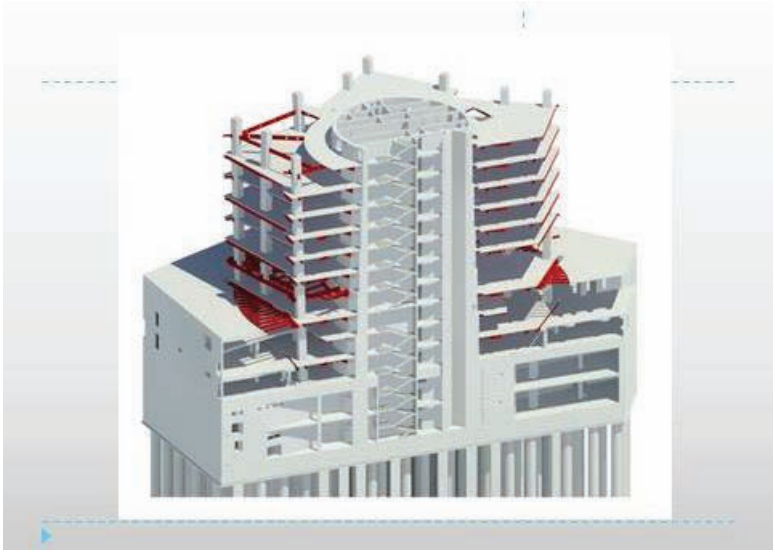

Figure 10. The aboveground part of the tower (Fragment).

The outer diameter of the core from the 8th to the 58th floor is 26.1 m; starting from the level of the 59th floor to the 80th floor, the outer diameter of the core decreases to 21.0 m.

5. DESIGNS OF STEEL-REINFORCED CONCRETE COLUMNS

Steel-reinforced concrete columns consist of a metal core, flexible reinforcement and concrete of class B80. The core material of the columns is HISTAR 460 Russia steel manufactured by ArcelorMittal. The cores of the columns are made of cross-section from HL series I-beams according to ASTM A6/A6M-12 and T-sections obtained by dividing of HL I-beams. Elements of the column core are welded with waist fillet welds (Figure 11).

In accordance with the architectural concept of the tower, steel-reinforced concrete columns are arranged in a spiral, thereby repeating the twisted surface of the building’s facade. The rotation of the axis of the metal core of the column is made at the levels of odd floors. The joint at the level of fracture of the core of the column is performed on the flange sheets. For direct transmission of the horizontal component of the force at the point of fracture of the axis of the column, this factory joint of the core of the column is performed at the level of the slab.

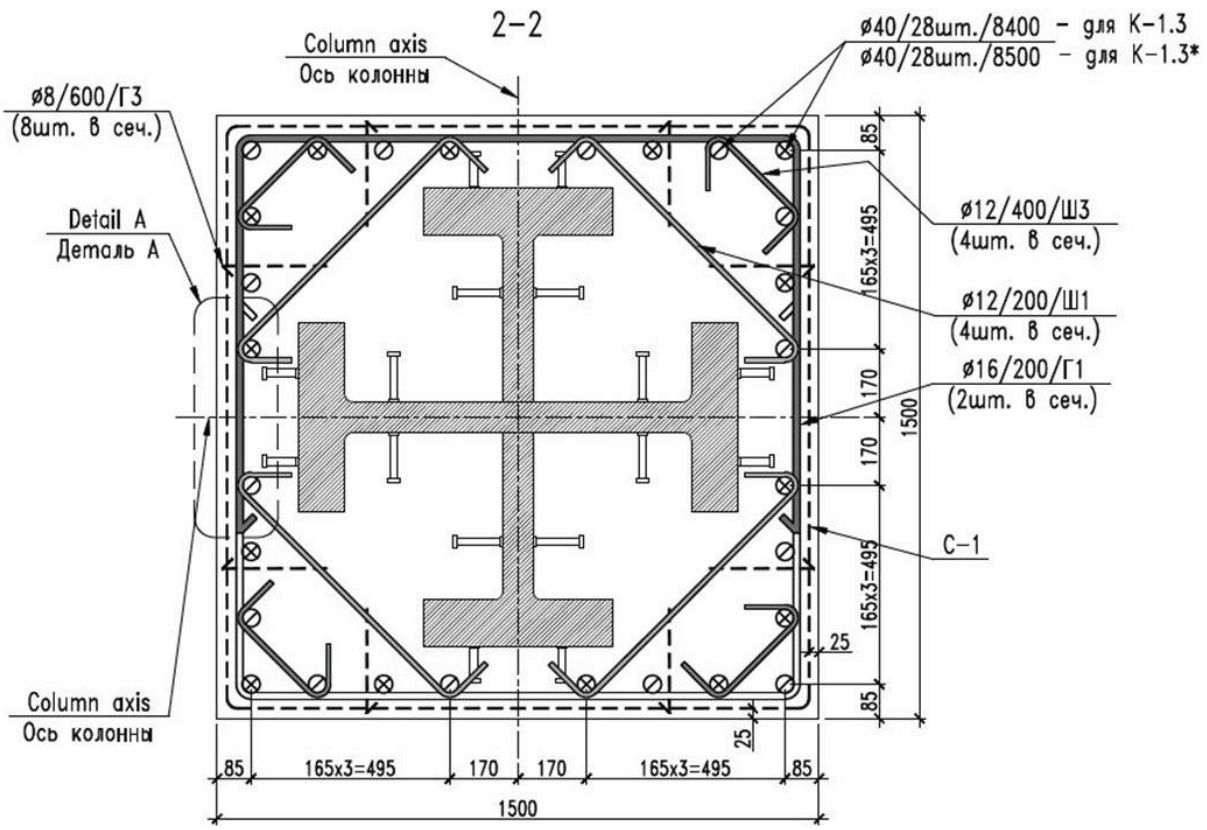

Figure 11. Column core of the tower.

The assembly joint of the column core is carried out in another place, 1200 mm above the floor slab. Mounting joints of metal cores are performed on bolts and are located every two floors of the building. The compressive forces in the assembly joints of the cores are transmitted through the milled ends of the elements, the tensile forces (occurring when calculating for progressive collapse) are transmitted through the lining of steel C345-3 on high-strength bolts M30 strength class 10.9.

To ensure the joint work of the steel core of the column with reinforced concrete, flexible stops (stud bolts) were installed on the core at the manufacturing plant.

In steel-reinforced concrete columns, concrete of class C80 for compressive strength is applied. For a relatively uniform transfer of the load more than 160,000 kN from the column to the foundation, the column base was developed, consisting of 7 plates, 40 mm thick. The space between the lower edge of the base of the column and the upper edge of the foundation slab was filled with high-strength material EMACO S55. Due to the fact that the column is tilted in the space around the steel base, a monolithic reinforced concrete box is arranged that perceives the horizontal component of the force in the column (Figure 12).

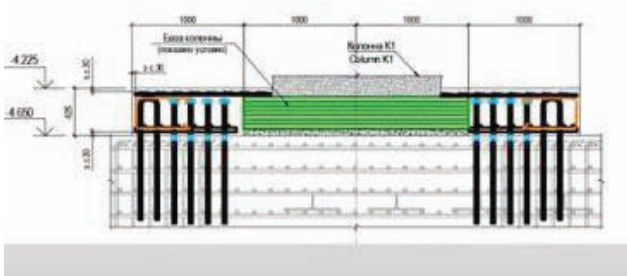

Figure 12. Concrete base coating.

Due to the fact that the ratio of the core diameter to the height of the building is about 1/17, the rigidity only of the core was not enough to satisfy the requirements of the norms for the horizontal deviation of the top of the building and the maximum acceleration of the oscillations of the upper floors (comfort of stay).

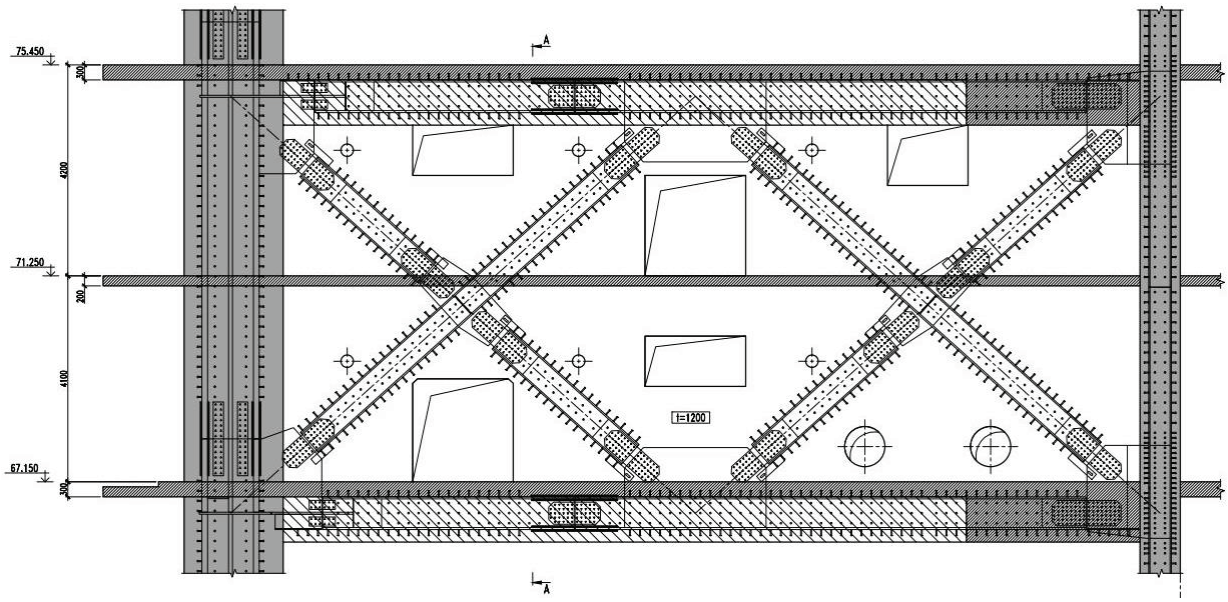

Figure 13. Connection of outriggers to core and columns.

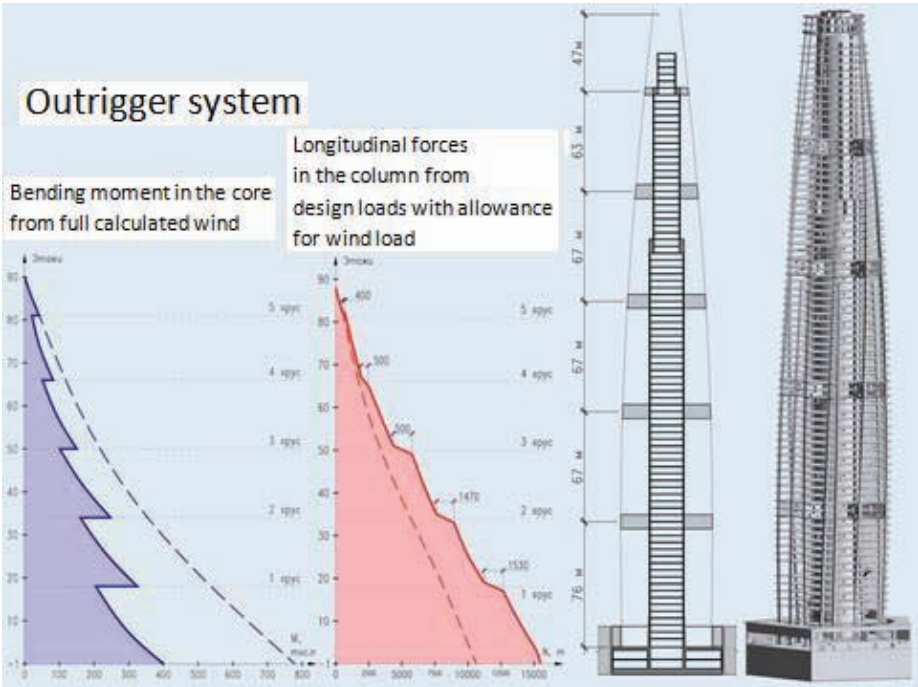

Figure 14. Outrigger system. Bending moment in the core from full calculated wind (left). Longitudinal forces in the column from design loads with allowance for wind load (right).

Additional rigidity of the building and its resistance to progressive collapse is provided by two-story outriggers located at the height of the tower at levels 17–18, 33–34, 49–50, and 65–66 technical floors (Figure 4). At each of these levels, outriggers are connected to core and 10 columns (Figure 13). The distribution plate above the 80th floor works as the top outrigger of the building. The introduction of outriggers made it possible to reduce the horizontal movement of the top of the building from the action of wind loads and to ensure the comfort of staying on the upper floors of the tower.

Figure 14 shows the values of bending moments in the central core, excluding and taking into account the inclusion of outriggers.

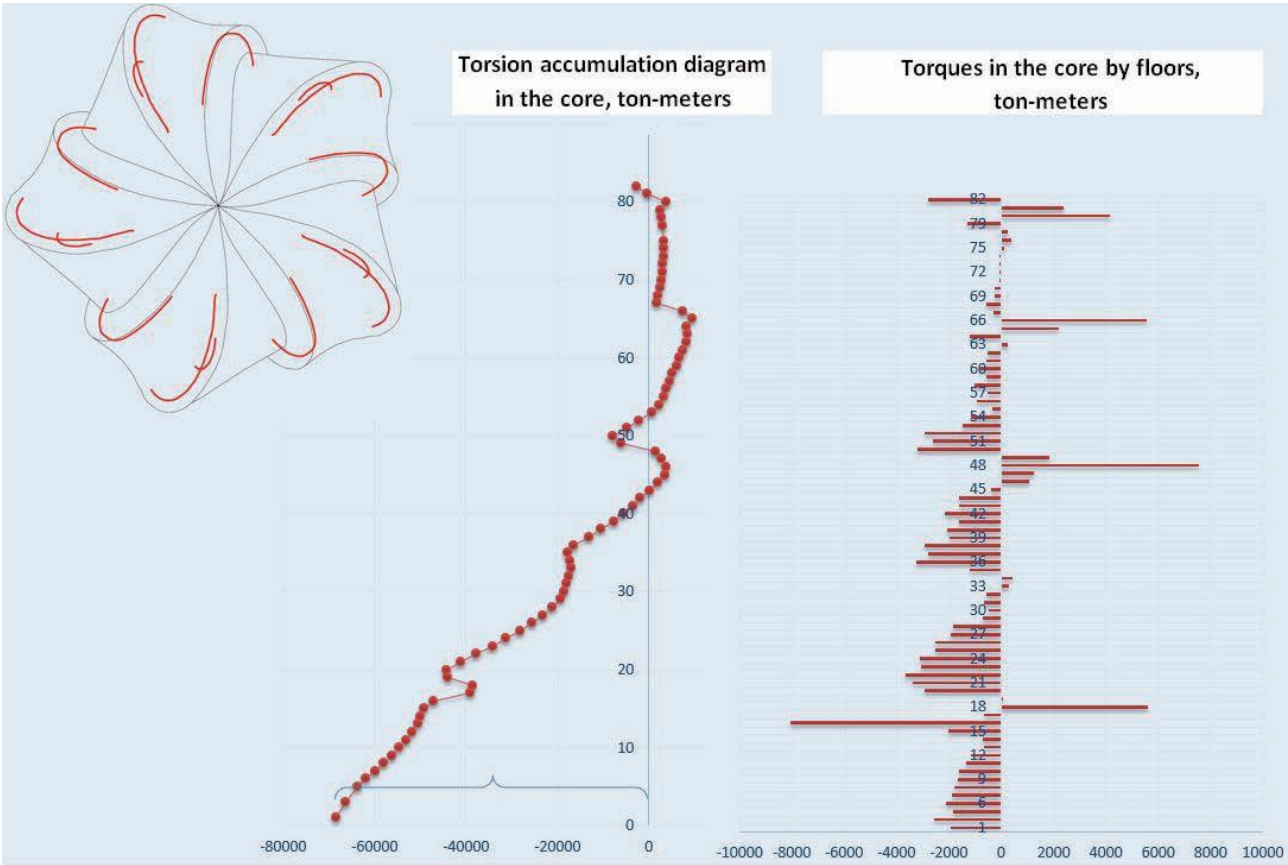

Figure 15. Torsion accumulation diagram in the core (left). Torques in the core by floors, ton-meters (right).

Outriggers are designed in the form of reinforced concrete beam walls, with steel trusses installed in the body of reinforced concrete. Steel trusses are designed for the perception of wind effects during the construction period of the building, before the inclusion of reinforced concrete outriggers.

As a result, the outrigger structures are an I-beam with the upper and lower shelves measuring 3.0x0.85 (h) meters and a wall of variable thickness (from 500 mm to 1500 mm in the adjoining zone to the core) 9.25 meters high. In order to strengthen the core at the level of adjacency of the upper and lower zones of the outrigger beam, annular monolithic reinforced concrete beams of size 2.5x1.2 (h) meters are made, in which openings are provided for passing vertical engineering communications.

Floor disks together with outrigger structures, provide joint spatial work of the main load-bearing structures of the building. In addition, due to the twisted shape of the building, the horizontal component of the forces from the fractures of the axes of the columns to the core of the building is transmitted through the floor disks. The structural design of the building leads to the accumulation of torque along the entire height of the central core. The maximum torque in the core at the level of its clamping in the upper plate of the box foundation is 770,000 kNm (Figure 15).

The walls of the central core of the tower were made of concrete of B80 compressive strength class.

6. DESIGN OF SLABS

The tower slabs outside the core are steel-reinforced concrete structures, made of in fixed formwork from a profiled steel sheets supported by metal beams.

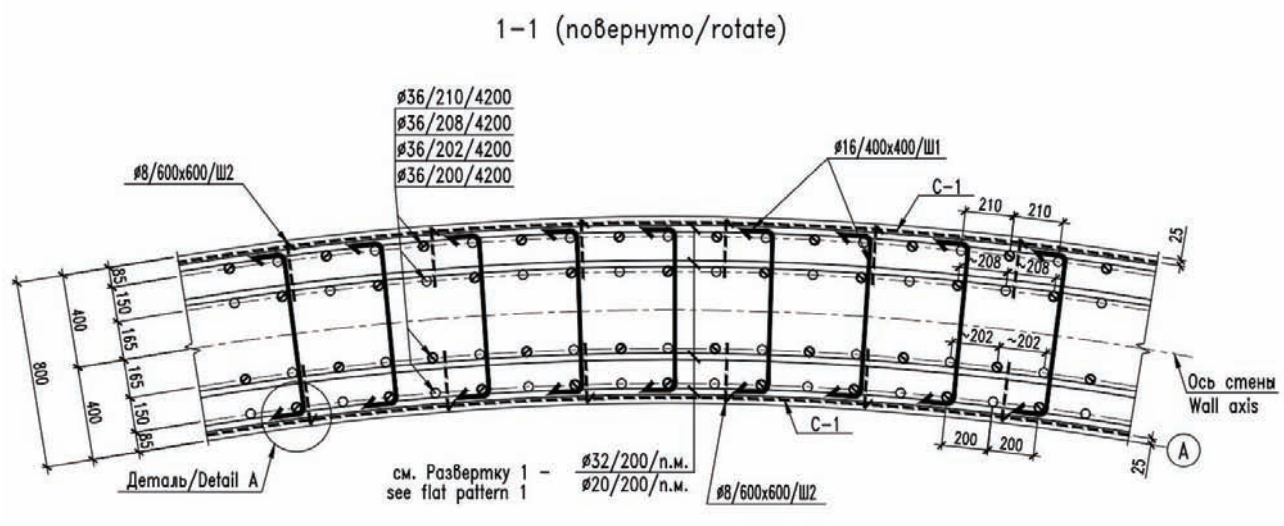

Figure 16. Fragment of reinforcing the wall of the central core.

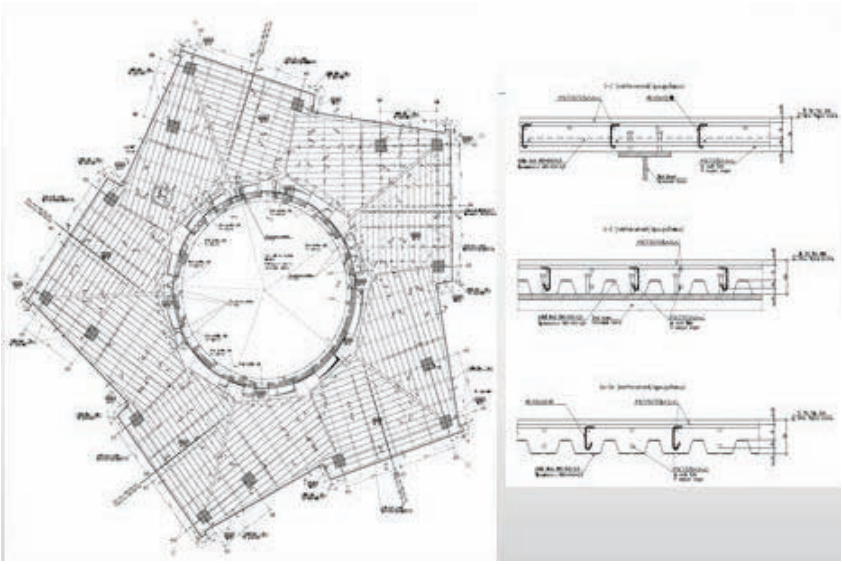

Figure 17. Floor slab design of a typical floor.

The thickness of such floor slabs is 150 mm, for which concrete of strength class B40 is used. Joint work of reinforced concrete floor slabs with metal floor beams is ensured by welding to the upper zones of the metal beams of flexible stops (studs) (Figure 17). The main I-beams located between the central core and the columns have a length of up to 17 m, they are made of welded, height from 750 to 1200 mm, secondary I-beams are made of rolled with sections up to 40B2 inclusive. The material of the metal beams is steel C345-3, C390. The nodes and mounting joints of the beams are frictional with high-strength bolts M24 of strength class 10.9 with controlled tension. The joining of the beams to the reinforced concrete structures of the central core is carried out using assembly welding to embedded parts.

Taking into account the architectural features of the building (a twisted spiral shape), each floor disk must perceive significant horizontal forces arising due to fractures in the axes of the columns and transmit constant general torsion forces to the core of the building. In this regard, it is provided:

- the use of intensified background reinforcement of a monolithic floor slab to transmit tensile and shear forces from inclined columns to the core of the building;
- the use of reinforcing cages and stud bolts, providing the transfer of global torsion efforts to the core of the building. The need for these frames is also caused by the presence of a large number of communication channels around the perimeter of the outer wall of the core.

The tower spire is functionally and constructively divided into two volumes:

- operated heated part, which is the completion of the volume of the tower and includes viewing platforms, elevators and ramps for lifting on them;
- the technical (unheated) part above the 87th floor mark, which has a front fence in the form of a steel mesh.
- The tower spire is designed in the form of a five-sided pyramid located around the central reinforced concrete core of the tower, and based on the overlapping of the 83rd floor at 344.400 m at the locations of the columns of the tower building. The height of the spire is about 118 meters, the width of the edge at the base of the spire pyramid is about 16.3 meters (Figure 18).

At the 87th floor mark (368.800 m) there is an overlap for the facade maintenance equipment, and at the 88th level mark (377.350 m) there is an overlap separating the lower exploited spire area from the upper technical one.

The spire is completed in the form of a steel pipe with a diameter of 1420 mm with a step-ladder located inside the spire to access the its top point.

The entrance block of the tower of 105 x 27m size is located in front of the building and is designed in the form of a front steel arch with a span of 105 m and has a coating made of steel supporting structures resting on the arch and on the main tower structures.

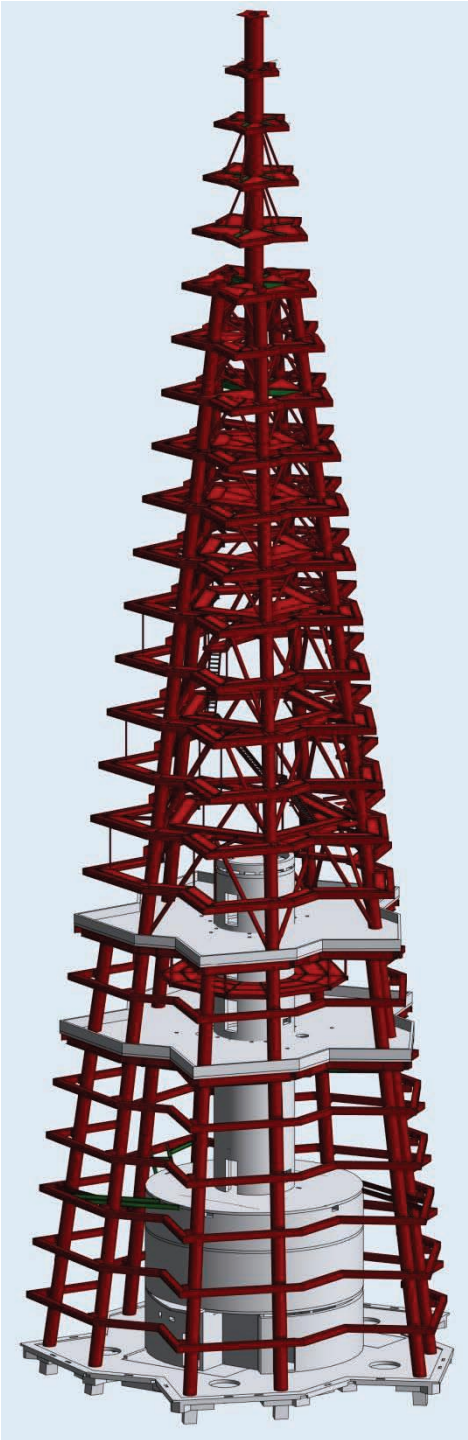

Figure 18. Spire pyramid.

The arch in its plane is glazed with the help of double-glazed windows, which are supported to the vertical load-bearing glass racks of variable height reaching 16.5 m and located along the arch with a step of 3.0 m. A section of the racks is 850 x 39.4 mm.

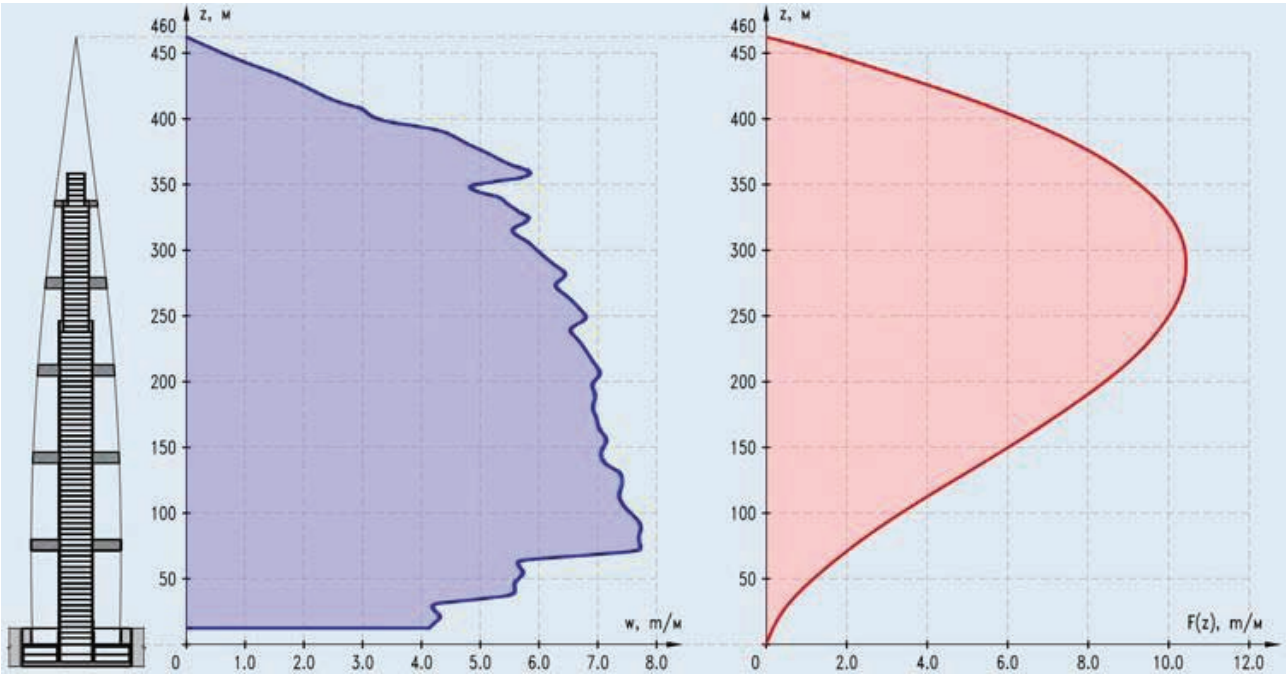

Figure 19. Wind loads.

They are glued from seven layers of heat-strengthened glass of 12 mm thick with a thickness of intermediate adhesive layers SG 0.89 mm.

7. STRUCTURAL ANALYSIS

In addition to gravitational loads, when conducting strutural analisys of the tower, wind loads were significant. The study of the model of the tower in the wind tunnel was performed by RWDI.

The aerodynamic coefficients of the total wind pressure *cp* as well as their distribution in plan in various sections along the height were determined.

The pulsation component of the wind load on the tower was determined on the basis of a dynamic calculation taking into account the value of the logarithmic decrement $\delta = 0.2$.

The maximum intensity values of wind loads, which must be taken into account when designing walling constructions and elements of their fastenings, were determined.

Special studies in the wind tunnel were carried out to determine the possible aerodynamically unstable oscillations of the tower. It turned out that with the accepted shape, size, rigidity and mass of the building, it did not undergo resonant vortex excitation or aerodynamic unstable vibrations such as galloping. In addition, the loss of aerodynamic stability such as divergence did not occur.

The surface ice loads acting on structural elements located at an altitude of 100 meters or more above the surface of the earth were also taken into account.

The sum of all horizontal forces from the action of the calculated wind load amounted to 48,360 kN, including the average component of the wind load - 30,790 kN and the pulsation component of the wind load - 17,580 kN (Figure 19). The value of the moment from the action of the full-calculated wind at the level of the top of the bottom plate of the box foundation is 9,379,000 kNm.

Modal analysis took into account about 100 modes of natural vibrations. The frequency in the first mode was 0.112 Hz. The total modal mass of the first eight modes of natural vibrations corresponds to approximately 75% of the total modal mass.

Figure 20 shows the first five modes of natural oscillations of the tower.

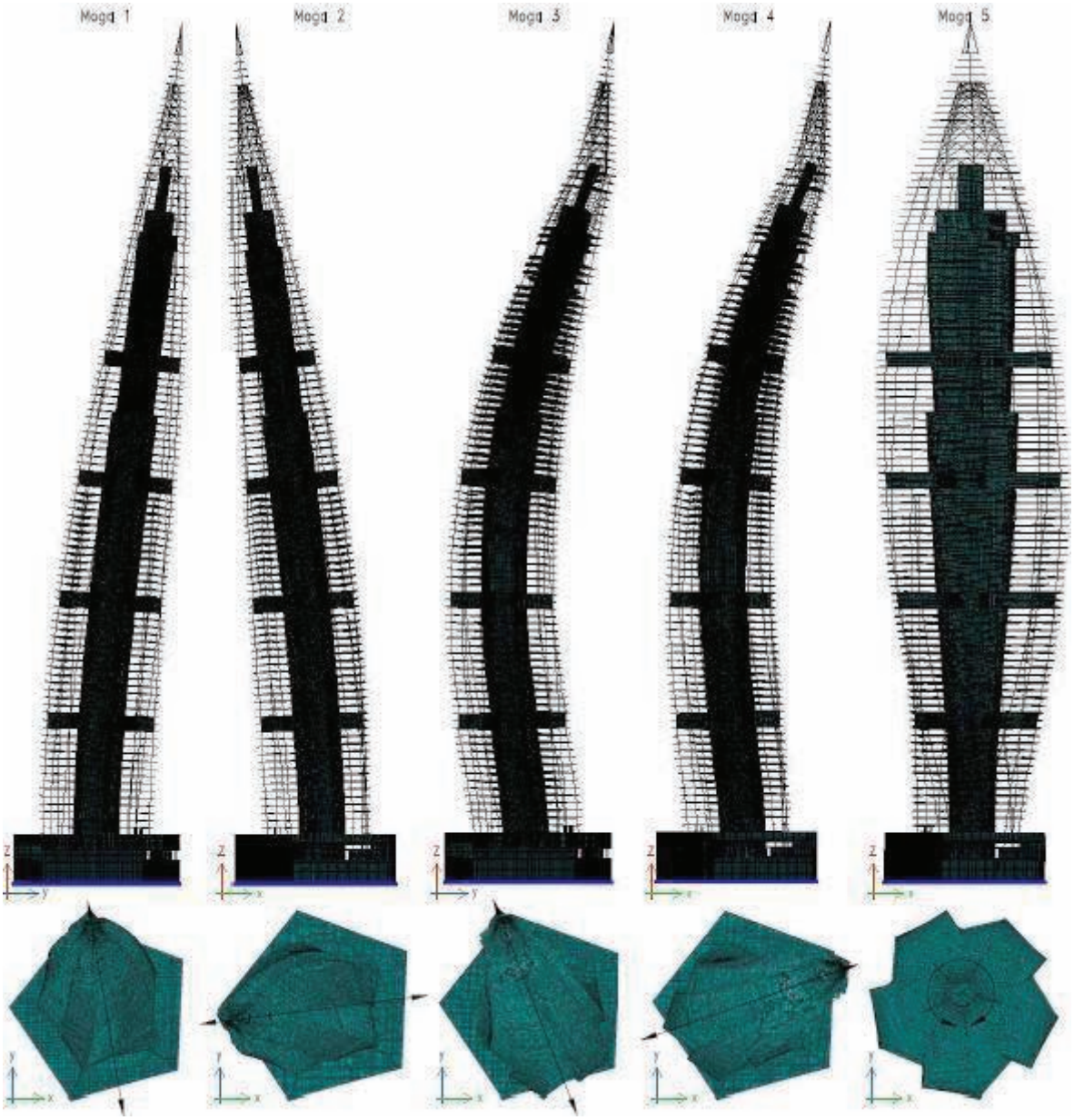

Figure 20. First five modes of natural oscillations of the tower.

The values of the horizontal displacement of the top and the acceleration of the vibrations of the top floors under wind pulsations are key indicators of the serviceability of a high-rise building.

Normative displacements under the components of the wind load at the level of the observation platform (mark 356.85 m) are 313 mm (1/1150 of the height of the building). The vibration acceleration, determined for the overlap of the upper office floor, was 0.0486 m / sec^2, which is 1.65 times lower than the maximum allowable vibration acceleration of the upper floors.

The design of such a unique building of a new architectural form, of great height, located on the coast of the Gulf of Finland in conditions of weak soils and unstable wind effects, with the development of new structural solutions using new construction materials, required a series of research works.

The test bases of TSNIISK named after V.A. Kucherenko, NIIZHB named after A.A. Gvozdev, NIIOSP named after N.M. Gersevanov, Perm National Research Polytechnic University, RWDI Laboratory (Canada) con-

ducted the following research studies of the Lakhta Center tower structures:

- The study of wind pressure and ice loads.
- Determination of soil properties.
- Tests of piles.
- Development of concrete compositions.
- Determination of the bearing capacity of steel-reinforced concrete columns.
- Tests of steel-reinforced concrete outriggers.
- Tests of glass load bearing columns.
- Development of the work technology.
- Monitoring.

We present the results of some of them.

8. AERODYNAMIC TESTS

The considering structure has a complex geometric shape, for which there are no values of the aerodynamic characteristics that need to assign the design wind loads acting on the load bearing and enclosing structures of the building and determine its aerodynamic stability. In order to determine the aerodynamic characteristics, the results of model aerodynamic tests conducted in the wind tunnel of RWDI (Canada) were used.

When designing the tower building, the following wind effects were found:

1. The average and pulsation components of the design wind load;
2. Peak values of the wind load acting on the structural elements of the fence;
3. The impact of wind on pedestrians in areas adjacent to the designed buildings.

Two design alternatives for the total wind load corresponding to the most unfavorable variants for loading the tower at wind acting angles of $\alpha = 190^\circ$ and 270°, were considered.

The figure shows the sections of the plan on floors 76 - 84 of the structure for which aerodynamic coefficients were determined by blowing in the wind tunnel.

Resonant vortex excitation is associated with the regular breakaway of vortices from the side surfaces of structures in areas of the building with weak conicity within which the cross-sectional size varies slightly. Based on the experience of blowing models of high-rise buildings and structures of various shapes in wind tunnels, it was found that for conical structures with a taper ≥ 0.15, wind resonance phenomena are not observed. For the considering building at heights z < 200 m, the average conicity of the building is 0.15, and above the conicity increases.

Aerodynamically unstable vibrations such as galloping can occur if the wind speed V exceeds a certain critical value $V_{cr,g}$, i.e. if

$$V > V_{cr,g} \equiv 2\, Sc\, f_1\, d/(-a_g\, \gamma_{cr})$$

and

$$a_g \equiv \left(\frac{dc_y}{d\alpha} + c_x \right) k_s < 0$$

In the above relations

$$Sc = 2m_1 \delta / (\rho_a d^2)$$

is Scruton number;

f_1 (Hz) is a frequency for i -th flexural natural vibration mode;

d (m) is a characteristic cross-section;

m_1 (kg/m) is an equivalent linear mass;

$\rho_a = 1.25$ kg/m^3 is density of air;

$\gamma_{cr} = 1.25$ is reliability coefficient;

$\delta = 0.07$ – logarithmic decrement for flexural vibrations of a building;

c_x and c_y are respectively, aerodynamic factors of frontal resistance and side force;

$k_s = 0.9$ is coefficient depending on vibration mode.

The results of tests in a wind tunnel showed that for the considering building, the coefficient $a_{g,max} = 0.92$ is achieved at heights close to 300 m.

After calculation we obtained that critical value of wind speed, for which unstable vibrations similar to galloping can appear, significantly exceeds wind speed at height z = 300 m. Consequently, aerodynamically unstable vibrations of galloping type do not arise in the considering building.

Figure 21. View of the Lakhta Center model in the RWDI wind tunnel.

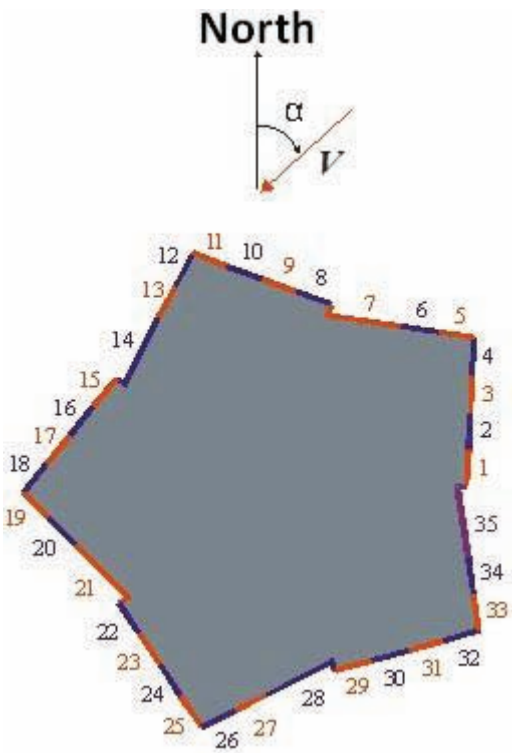

Figure 22. The scheme of locations of zones of the tower; floors 76-84.

Critical wind velocity, for which torsion unstable vibrations of divergence type arise, can be determined by the following formula

$$v_{div} = \sqrt{\frac{2G_t}{\rho d^2 dc_m / d\alpha}},$$

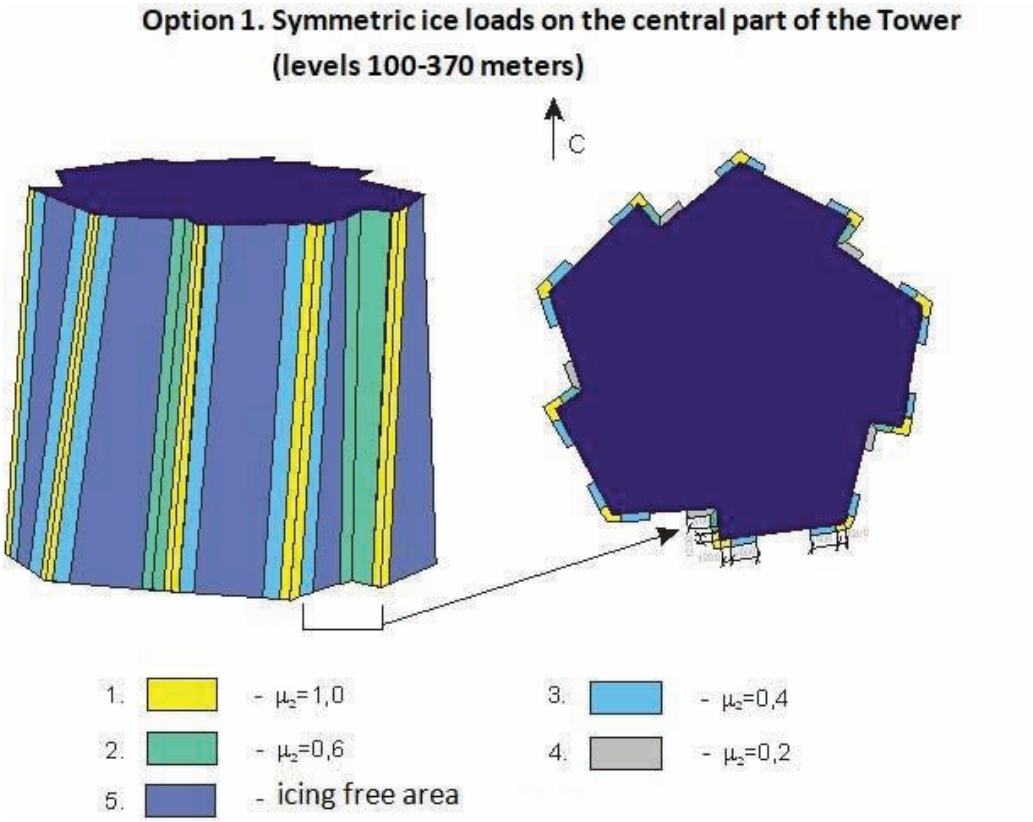

Figure 23. Ice loads (the first option).

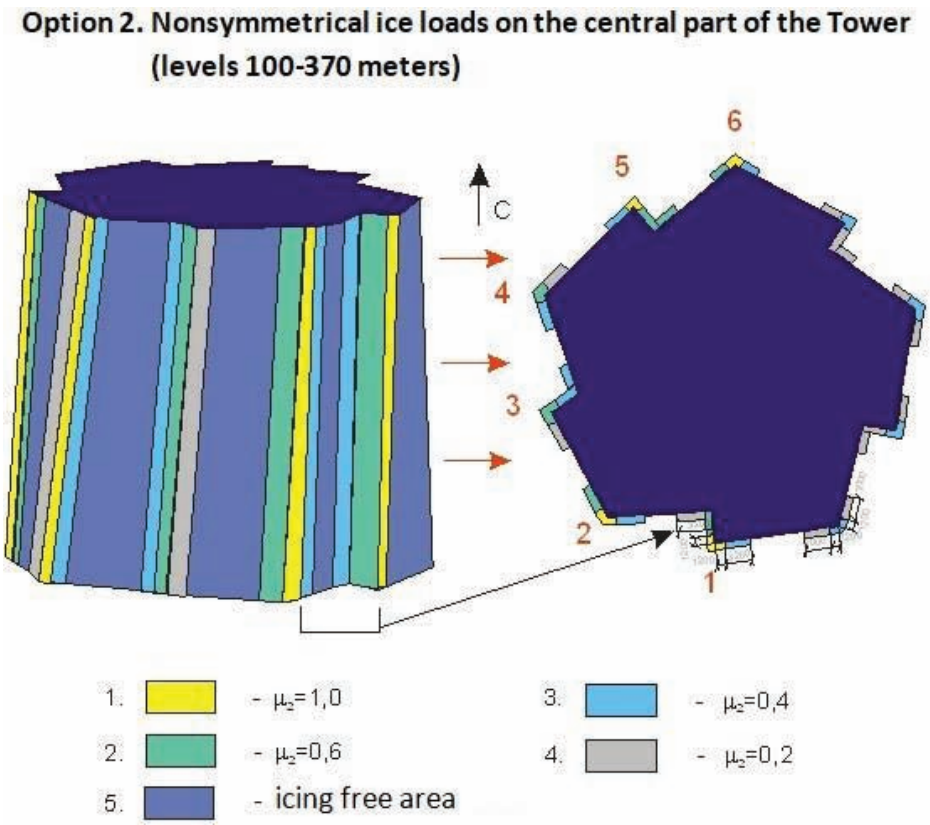

Figure 24. Ice loads (the second option).

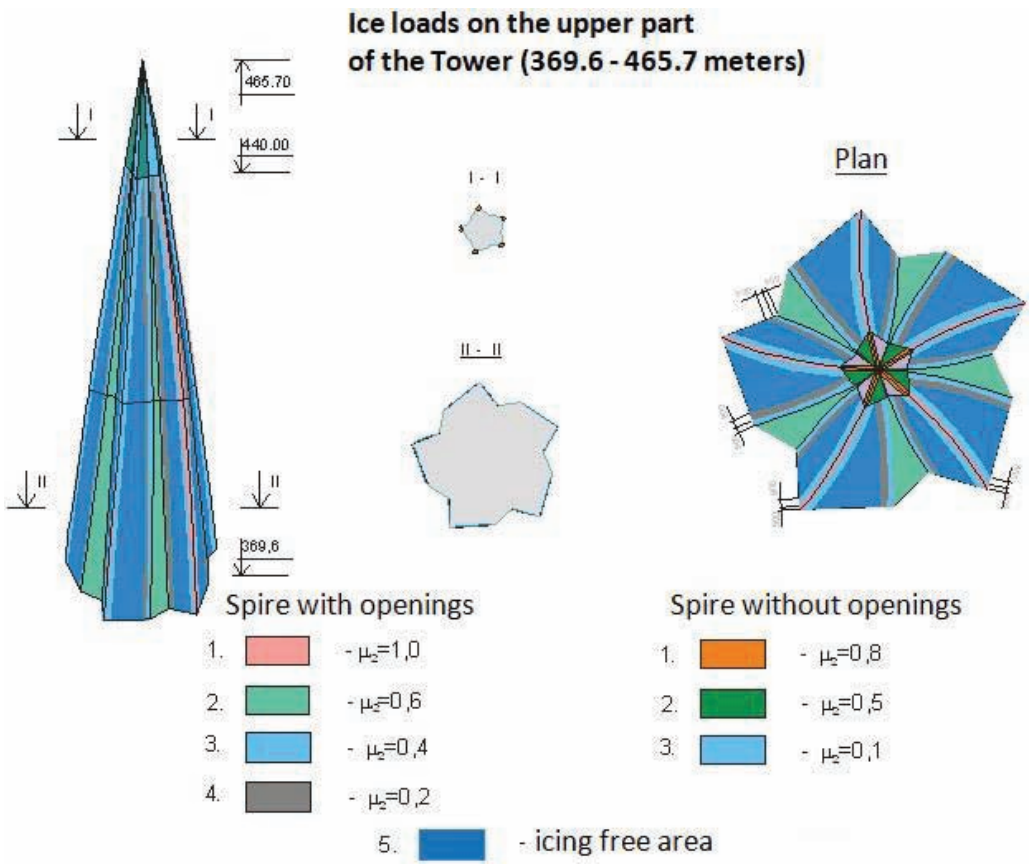

Figure 25. Ice loads.

where G_t is a torsion rigidity of a structure;
$dc_m/d\alpha$ is a gradient of moment coefficient c_m change in accordance with attack angle α.
The results of model tests in a wind tunnel showed that the coefficients c_m and $dc_m/d\alpha$ are close to zero, which eliminates the loss of aerodynamic stability such as divergence in the considering building.

9. ABOUT ICE LOAD

Since the tower building is located in low cloudy conditions when calculating it, the surface ice loads acting on structural elements located at an altitude of 100 or more meters above the ground were taken into account. The symmetric and asymmetric loading of the building surface of the tower was taken into account by the ice load.

10. ENGINEERING-GEOLOGICAL RESEARCH

In order to study the Vendian deposits, special researches were conducted, as a result of which it was established:

- the deformation modulus varies with depth;
- clays are over-compacted OCR = 2 ... 3;
- clay has a strongly expressed anisotropy
- clay has creep.

The highest values both in absolute value and in the rate of change with depth were obtained as a result of pressiometric tests, in which the deformation modulus changed from 100 MPa (at a depth of 35 m) to 560 MPa (95 m), i.e. 5.6 times. Studies of the effect of soil compaction on the foundation sediment showed that when the soil compaction coefficient (OCR) changes from 1 to 1.5, there is a sharp decrease of sediments for 25%, from 0.2 to 0.15 m, in the future it gradually decreases uniformly from 0,15 to 0.12 m when OCR changes from 1.5 to 4.

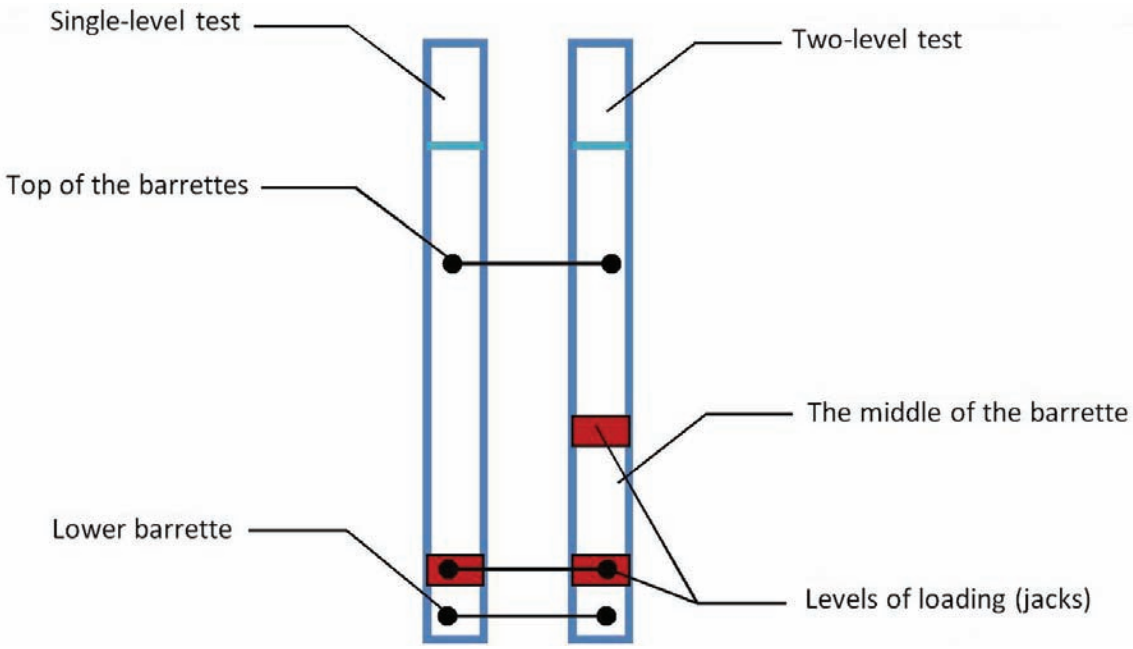

Figure 26. Scheme of barrettes.

In order to study the creep of the soil, corresponding laboratory tests were carried out. Such tests made it possible to reveal the dependence of the secondary consolidation coefficient on the load. The obtained values of creep were specified in the process of field stamp tests. The lower parts of piles and barrettes served as stamps. As a result of the studies, it was determined that additional sediment due to creep of the soil is 30%.

In order to study the interaction of the barrettes with each other and with the soil in a pile field, special geotechnical studies were carried out. It consisted of testing five barrettes with a working length of 65 m and a cross section of 1.5 × 2.8 m. Three of the five tested barrettes were subjected to a group test, in which loading was carried out simultaneously.

The submersible jacks were chosen for testing. Among the five tested barrettes, three were equipped with loading devices installed in two levels, and two barrettes had a single one, in one level. Schemes of one-level and two-level tests and the accepted names of the parts of the barrettes are shown in the Figure 26.

The study of the stress distribution along the length of the barrette during loading of the lower and upper level jacks showed that the greatest attenuation of the forces is along the length, and therefore the greatest resistance along the lateral surface was observed for the central barrette B2.

A set of studies of weak soils for the possibility of building high-rise buildings on them allowed us to obtain a number of important results that can be used in similar cases, as well as included in the newly developed Building Codes.

11. TESTING OF STEEL-REINFORCED CONCRETE COLUMNS

When developing the project, it was initially intended to use reinforced concrete columns made of high-strength concrete. However, the cross-sectional dimensions turned out to be very large, which led to the loss of usable floor area. Therefore, it was proposed to use steel-reinforced concrete columns. The use of such columns made of high-strength concrete and new classes of high-strength steel allowed significantly increasing the useful area of the building. Due to the absence of design standards for such structures in the Russian Federation, experimental and theoretical studies of specimens of columns with rigid reinforcement in the form of

welded I-beams for central and eccentric compression, as well as for shear, were carried out.

Firstly, full-scale experiments on central and eccentric compression of column models were carried out. Totally, 44 specimens made of B80 concrete, fiber-reinforced concrete and C255 steel were tested.

As a result of tests under the compressive load, the dependences of stresses and strains in the steel core and concrete were obtained. The effect of the eccentricities of the load application and a large percentage of reinforcement from 10% to 18% when using high-strength concrete on the bearing capacity was studied.

The destruction of concrete prisms was characterized by a sharp loss of bearing capacity and brittle destruction with clapping. Fiber-reinforced concrete was characterized by a gradual decreasing the deformation modulus, a gradual accumulation of cracks.

The destruction of samples even with significant eccentricities occurred smoothly due to the plastic properties of steel.

When testing models made of concrete B80 and fiber-reinforced concrete, the actual ratio of the distribution of stresses, strains and forces between rigid reinforcement and concrete at each step of loading was established.

In order to detailed study of the process of deforming and fracture of the composite column structure and comparison with experimental results, numerical simulation of the tested specimens was performed using the finite element method by the ANSYS software.

The calculations were carried out in linear and nonlinear formulations.

The real characteristics of the materials obtained in the experiments were used. Rigid reinforcement and concrete were modeled by volumetric elements, flexible reinforcement simulated by rod elements.

The results of a linear calculation for central and eccentric compression showed that the stresses in concrete in certain zones exceed the limit values, which contributes to the appearance of cracks, and plastic deformations can appear in rigid reinforcement.

Therefore, a calculation that takes into account the nonlinear properties of concrete and steel was conducted.

Comparison of the experimental results with the calculation showed fairly close values, and the normative technique provides a large safety factor.

The presence of eccentricities under the action of the load on the column causes the appearance of bending moments in the structure and can cause a violation of the adhesion between concrete and rigid reinforcement.

Shear tests were performed to find out this fact. The main goal of such tests was to determine the parameters of the beginning of bond fracture, and the type of fracture in the steel-concrete contact zone when pressing rigid reinforcement into concrete, as well as the study of the possibility of increasing the adhesion strength in the contact zone.

The adhesion strength between the series of specimens differed slightly. For series of specimens made of concrete B80 and fiber-reinforced concrete, the following facts should be noted: concrete B80 was mainly characterized by a sharp breakdown of the contact surface, and fiber-reinforced concrete was characterized by a gradual decrease in its bearing capacity.

Fiber concrete collapsed with the formation of “ripped” and “hairy” cracks with exposure of steel fiber.

When the length of the steel-concrete contact zone was increased 1.5 times, the maximum load for separation of concrete from reinforcement increased almost proportionally.

Strengthening of rigid reinforcement with longitudinal re-bars in fiber reinforced concrete specimens practically did not lead to an increase in adhesion strength.

In order to justify the results of the experiments and to predict correctly the beginning of bond breaking in the contact zone, the boundary-value problem was solved taking into account the contact interaction of elements in the structure using the finite element method.

At the joint steel-concrete boundary, the normal and tangent components of the distributed contact force arise.

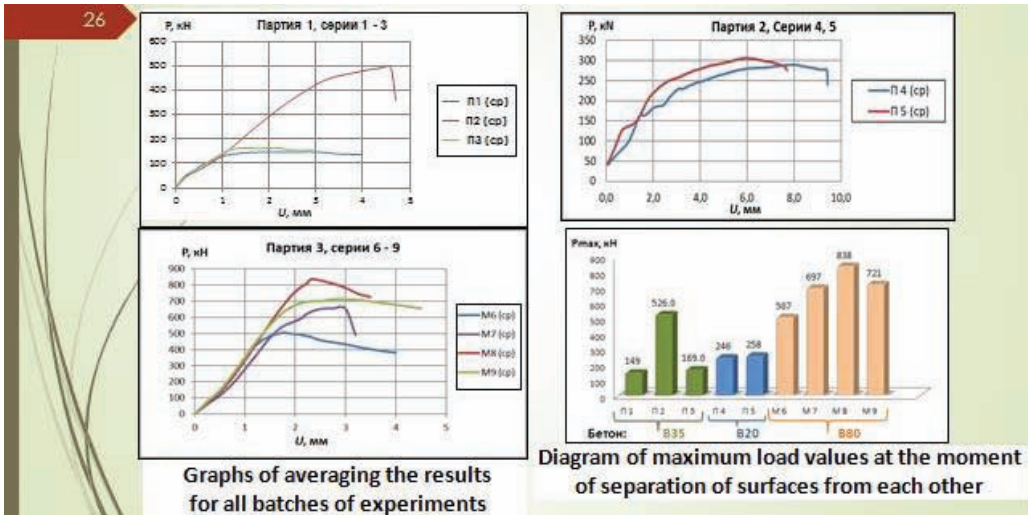

Figure 27. Shear Test Results.
Graphs of averaging the results for all batches of experiments (left).
Diagram of maximum load values at the moment of separation of surfaces from each other (right)).

While the bodies are glued together, the tangential forces do not depend on the normal contact forces, but when the bodies loss the contact, the shear begins.

The most important issue when modeling contact problems is the correct choice of a mathematical model for the interaction of contacting surfaces. The separation mechanism of bonded surfaces was modeled by contact elements. When constructing the finite element model, the symmetry of the computational domain was taken into account. The calculation was carried out on a quarter of the sample model. Different mesh options were considered. The problem was solved in linear and nonlinear formulations.

As a result, it was concluded that the geometric shape of rigid reinforcement affects the process of mechanical adhesion in the contact zone. The calculation results were in good agreement with the experimental results, and numerical modeling allowed us to determine the stress-strain state in the contact zone in an arbitrary point of rigid reinforcement, which changes during loading.

Taking into account the nonlinear properties of concrete made it possible to obtain a picture of crack formation with increasing load. Taking into account the nonlinear properties of steel showed the appearance and development of zones of plastic deformations in rigid reinforcement. The stresses in concrete and reinforcement for the given classes of concrete and reinforcement turned out to be lower than the calculated values, (with the exception of special points).

The influence of the geometry of the profile of rigid reinforcement on the load distribution between the elements of the steel-reinforced concrete column was also studied. Three versions of columns with the same cross-sectional area of concrete, flexible and rigid reinforcement were considered. A nonlinear calculation was performed, and the loads were determined when cracks in concrete and plastic deformations in the metal appeared. The calculation showed that rigid reinforcement made of two cross-mounted I-beams is able to provide a bearing capacity of up to 210,000 kN for the accepted section sizes, and it is the most rational among the considered variants.

12. GLASS RACKS

Tests on 18 samples of three groups of models of laminated heat-strengthened glass of rectangular cross-section were conducted. The first group of models was equivalent to full-scale facade racks in flexibility in both planes and was tested by central and eccentric compression with a given eccentricity.

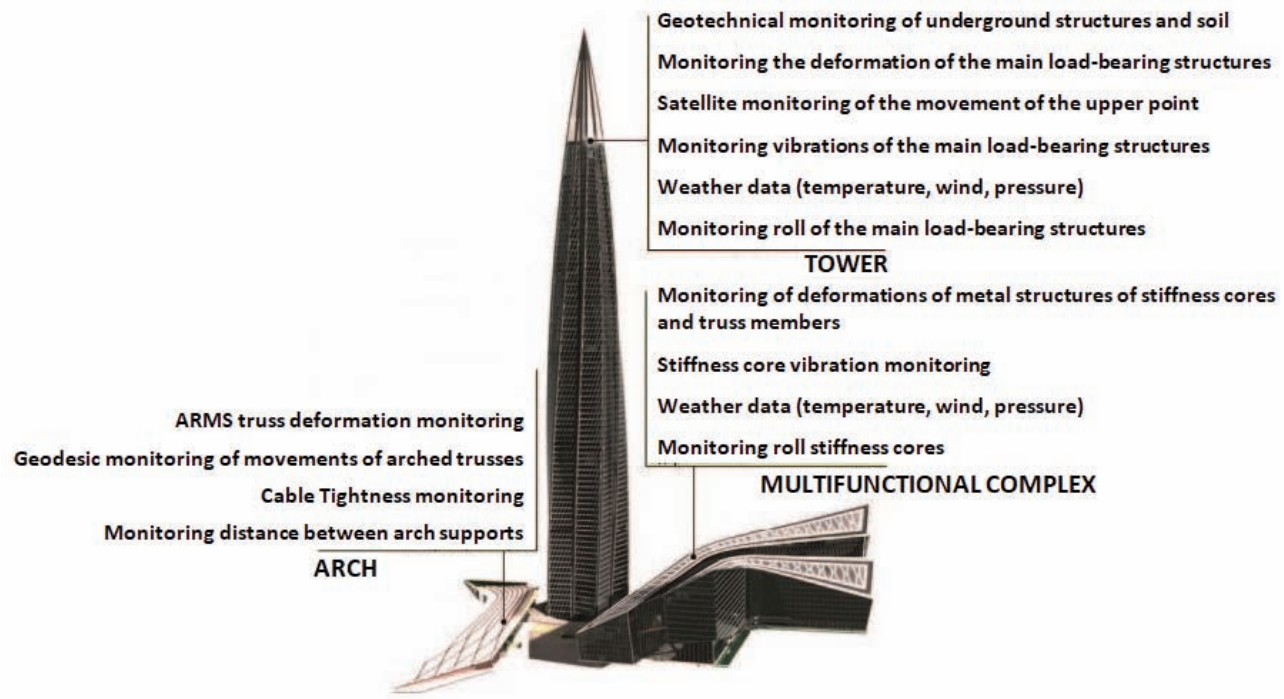

Figure 27. About structural health monitoring of the tower.

The second group of models was tested for pure bending. The third group of models was tested by central compression. Glasses for all models were heat-strengthened of 12 mm thick, adhesive layers of 0.89 mm thick. When testing models for compression, the hinge work of the upper and lower supports of the racks, the studied eccentricity, as well as the simple supporting for the beams were provided.

As a result of the tests, the values of breaking loads for the initial failure (by the appearance of the first crack) and complete destruction were obtained. Complete destruction of flexible rack specimens under normal loading occurred after loss of stability. When testing specimens of short beams, complete failure occurred immediately after the first cracks appeared. Centrally compressed prisms of low flexibility are characterized by a large difference between the initial and complete fracture stresses (1.4 ... 2.8 times).

The elastic modulus values of glass multilayer specimens differed for the main axes of the section and took the values: in the direction normal to the glass layers - 30,000 MPa; along the glass layers - 60,000 MPa. An elastic modulus of 12,500 MPa was accepted to calculate the deformations of glass structures.

13. STRUCTURAL HEALTH MONITORING

In accordance with the current regulatory documents, in order to ensure erection and operation safety of unique buildings as part of the scientific and technical support (STS) of construction, a set of measures was organized to continuously monitor the stress-strain state (SSS) of structures.

The main purpose of monitoring is minimizing of the possibility of emergencies caused by uncertainties in the work of the load bearing structures of a building and a soil of the foundation.

The development of the monitoring program for the foundations and the aboveground parts of the tower was carried out by specialists of SAMSUNG C&T, CJSC GORPROEKT, SODIS LAB, INFORSPROEKT, and NIIOSP named after N.M. Gersevanov in 2015 [4] (Figure 28 and Figure 29).

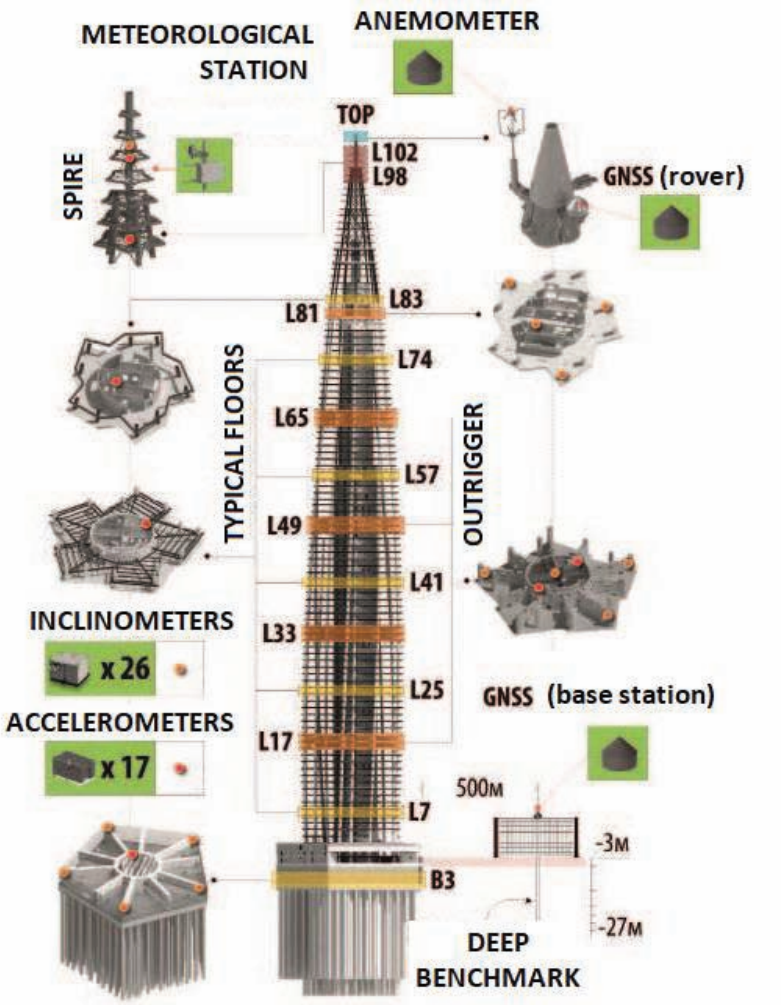

Figure 28. About structural health monitoring of the tower.

In order to control the stress-strain state, totally 1210 string strain gauges were installed in 196 targets on the rods of the working reinforcement of the lower plate, diaphragm walls and upper plate.

The aboveground part of the tower was equipped with an automated system for monitoring relative deformations. It consists of 1257 string strain gauges of various types. With their help, measurements are made of the axial deformations of composite columns on typical floors, vertical and horizontal deformations of the walls of the reinforced concrete core, comprehensive monitoring of the deformation of outrigger trusses and steel structures of the spire.

Real-time monitoring and post-processing planning of horizontal and vertical movements of the upper point of the building is carried out using a satellite geodetic monitoring system [5-10]. Satellite monitoring of the movement of the upper point, together with the results of monitoring of rolls and vibrations, provides comprehensive information about the deformation of the axis of the building.

Two weather stations allow conducting of a correlation analysis of the stress-strain state parameters and separating the changes in parameters associated with the degradation of building structures and seasonal and climatic changes.

REFERENCES

1. **Travush V.I., Shakhvorostov A.I.** Betonirovaniye nizhney plity korobchatogo fundamenta kompleksa «Lakhta tsentr» [Concreting of the bottom slab of the box-shaped

foundation of the Lakhta Center complex]. // *Vysotnyye zdaniya*, 2015, No. 1, pp. 92-101 (in Russian).

2. **Travush V.I., Konin D.V., Rozhkova L.S., Krylov A.S., Kaprielov S.S., Chilin I.A., Martirosyan A.S., Fim kin A.I.** Eksperimental'nyye issledovaniya stalezhelezobetonnykh konstruktsiy na vnetsentrennoye szhatiye [Experimental studies of steel-reinforced concrete structures for eccentric compression]. // *Academia. Arkhitektura i stroitel'stvo*, 2016, No 3, pp.127-135 (in Russian).
3. SP 63.13330.2012. Betonnyye i zhelezobetonnyye konstruktsii. Osnovnyye polozheniya [Concrete and reinforced concrete structures. The main provisions]. Design Code of the Russian Federation. Moscow, 2013 (in Russian).
4. **Travush V.I., Shakhraman'yan A.M., Kolotovichev YU.A., Shakhvorostov A.I., Desyatkin M.V., Shulyat'yev O.A., Shulyat'yev S.O.** "Lakhta tsentr" avtomatizirovannyy monitoring deformatsiy nesushchikh konstruktsiy i osnovaniya [Lakhta Center automated monitoring of deformations of load-bearing structures and foundations]. // *Academia. Arkhitektura i stroitel'stvo*, 2018, No. 4, pp. 94-108 (in Russian).
5. **Belostotsky A.M., Akimov P.A., Afanasyeva I.N., Kaytukov T.B.** Contemporary Problems of Numerical Modelling of Unique Structures and Buildings. // *International Journal for Computational Civil and Structural Engineering*, 2017, Volume 13, Issue 2, pp. 9-34.
6. **Belostotsky A.M., Akimov P.A.** Nauchnoissledovatelsky tsentr StaDyO. 25 let na fronte chislennogo modelirovaniys [25-th Anniversary of scientific research centre StaDyO]. // *International Journal for Computational Civil and Structural Engineering*, 2016, Volume 12, Issue 1, pp. 9-34 (in Russian).
7. **Belostotsky A.M., Akimov P.A.** O voprosakh avtomatizatsii system monitoring dlya otsenki tekuschego sostoyaniya stroitelnikh konstruktsiy zdaniy i sooruzheniy [About Automation of Structural Health Monitoring Systems]. // *International Journal for Computational Civil and Structural Engineering*, 2016, Volume 12, Issue 3, pp. 26-34 (in Russian).
8. **Ilyukhina E.A., Lahman S.I., Miller A.B., Travush V.I.** Konstruktivnye reshenija vysotnogo zdanija "Lahta Centr" v Sankt-Peterburge [Design Solutions of the High-Rise Building "Lakhta Center" in Saint-Petersburg]. // *Academia. Arkhitektura i stroitel'stvo*, 2019, No. 3, pp. 110-121 (in Russian).
9. **Travush V.I., Belostotsky A.M., Akimov P.A.** Contemporary Digital Technologies in Construction. Part 1: About Mathematical (Numerical) Modelling. // *IOP Conference Series: Materials Science and Engineering*, 2018, Volume 456, conference 1, 012029.
10. **Travush V.I., Belostotsky A.M., Akimov P.A.** Contemporary Digital Technologies in Construction. Part 2: About Experimental & Field Studies, Material Sciences, Construction Operations, BIM and "Smart" City. // *IOP Conference Series: Materials Science and Engineering*, 2018, Volume 456, conference 1, 012030.

СПИСОК ЛИТЕРАТУРЫ

1. **Травуш В.И., Шахворостов А.И.** Бетонирование нижней плиты коробчатого фундамента комплекса «Лахта центр». // Высотные здания, 2015, №1, с.92-101.
2. **Травуш В.И., Конин Д.В., Рожкова Л.С., Крылов А.С., Каприелов С.С., Чилин И.А., Мартиросян А.С., Фимкин А.И.** Экспериментальные исследования сталежелезобетонных конструкций на внецентренное сжатие. // *Academia. Архитектура и строительство*, 2016, №3, с. 127-135.
3. СП 63.13330.2012. Бетонные и железобетонные конструкции. Основные положения. – М., 2013.

4. **Травуш В.И., Шахраманьян А.М., Колотовичев Ю.А., Шахворостов А.И.. Десяткин М.В., Шулятьев О.А., Шулятьев С.О.** «Лахта центр» автоматизированный мониторинг деформаций несущих конструкций и основания. // *Academia. Архитектура и строительство*, 2018, №4, с. 94-108.
5. **Belostotsky A.M., Akimov P.A., Afanasyeva I.N., Kaytukov T.B.** Contemporary Problems of Numerical Modelling of Unique Structures and Buildings. // *International Journal for Computational Civil and Structural Engineering*, 2017, Volume 13, Issue 2, pp. 9-34.
6. **Белостоцкий А.М., Акимов П.А.** Научно-исследовательский центр СтаДиО. 25 лет на фронте численного моделирования. // *International Journal for Computational Civil and Structural Engineering*, 2016, Volume 12, Issue 1, pp. 9-34.
7. **Белостоцкий А.М., Акимов П.А.** О вопросах автоматизации систем мониторинга для оценки текущего состояния строительных конструкций, зданий и сооружений. // *International Journal for Computational Civil and Structural Engineering*, 2016, Volume 12, Issue 3, pp. 26-34.
8. **Илюхина Е.А., Лахман С.И., Миллер А.Б., Травуш В.И.** Конструктивные решения высотного здания «Лахта центр» в Санкт-Петербурге. // *Academia. Архитектура и строительство*, 2019, №3, с. 110-121.
9. **Travush V.I., Belostotsky A.M., Akimov P.A.** Contemporary Digital Technologies in Construction. Part 1: About Mathematical (Numerical) Modelling. // *IOP Conference Series: Materials Science and Engineering*, 2018, Volume 456, conference 1, 012029.
10. **Travush V.I., Belostotsky A.M., Akimov P.A.** Contemporary Digital Technologies in Construction. Part 2: About Experimental & Field Studies, Material Sciences, Construction Operations, BIM and “Smart” City. // *IOP Conference Series: Materials Science and Engineering*, 2018, Volume 456, conference 1, 012030.

Илюхина Елена Анатольевна, кандидат экономических наук; генеральный директор, Акционерное общество «Многофункциональный комплекс «Лахта центр»; 190000, Россия, г. Санкт-Петербург, ул. Почтамтская, д. 3-5, литер «А», ч.пом. 1Н, ком. 370;
тел. +7 (800) 700-31-52.

Лахман Сергей Ильич, кандидат экономических наук; генеральный директор, закрытое акционерное общество «Городской проектный институт жилых и общественных зданий»; 105064, Россия, г. Москва, Нижний Сусальный переулок, д.5, стр. 5А;
тел./факс +7 (495) 775-75-65;
E-mail: info@gorproject.ru.

Миллер Алексей Борисович, кандидат экономических наук; председатель правления, публичное акционерное общество «Газпром»; 117997, Россия, ГСП-7, г. Москва, ул. Наметкина, д. 16; тел. +7 (495) 719-21-09;
факсы: +7(495) 719-83-33, +7(812) 413-73-33;
E-mail: gazprom@gazprom.ru.

Травуш Владимир Ильич, академик РААСН, доктор технических наук, профессор; вице-президент Российской академии архитектуры и строительных наук; заместитель генерального директора, закрытое акционерное общество «Городской проектный институт жилых и общественных зданий»; 105064, Россия, г. Москва, Нижний Сусальный переулок, д.5, стр. 5А;
тел./факс: +7 (495) 775-75-65, +7(495) 909-39-39;
E-mail: travush@mail.ru.

Elena A. Ilyukhina, Ph.D., General Director, Joint Stock Company “Multifunctional complex Lakhta Center”; 3-5, ul. Pochtamtskaya, Saint-Petersburg, 190000, Russia; phone: +7(800) 700-31-52.

Sergey I. Lakhman, Ph.D., General Director of City Design Institute for Residential and Public Buildings; building 5A, 5, Nizhny Susalny pereulok, Moscow, 105064, Russia; phone/fax: +7 (495) 775-75-65;
E-mail: info@gorproject.ru.

Alexey B. Miller, Ph.D., Chairman of the Management Committee of public joint stock company “Gazprom”; 16, ul. Nametkina, Moscow, 117997, Russia;
fax: +7(495) 719-83-33, +7(812) 413-73-33;
E-mail: gazprom@gazprom.ru.

Vladimir I. Travush, Full Member of the Russian Academy of Architecture and Construction Sciences, Professor, Dr.Sc., Vice-President of the Russian Academy of Architecture and Construction Sciences; Vice-Director of City Design Institute for Residential and Public Buildings; building 5A, 5, Nizhny Susalny pereulok, Moscow, 105064, Russia; phone/fax: +7 (495) 775-75-65,
909-39-39; e-mail: travush@mail.ru.